Scaling Techniques Using CFD and Wind Tunnel Measurements for use in Aircraft Design

Karl Pettersson

September 2006

Licentiate Thesis
Department of Aeronautical and Vehicle Engineering
Division of Aerodynamics
SE-100 44 Stockholm, Sweden
TRITA-AVE 2006:64
ISSN 1651-7660

Akademisk avhandling som med tillstånd av Kungliga Tekniska Högskolan i Stockholm framlägges till offentlig granskning för avläggande av teknologie licentiatexamen fredagen den 13:e Oktober kl 10:00 i Sal S40, Kungliga Tekniska Högskolan, Teknikringen 8, Stockholm.

Universitetsservice US AB, Stockholm 2006

Preface

This work was carried out at the Department of Aeronautical and Vehicle Engineering. The financial support to this work was provided by the REMFI project (contract AST3-CT-2004-502895), 6^{th} EU framework programme and is gratefully acknowledged. SNIC and PDC are also acknowledged for their help and support with the parallel computer on which these calculations have been done.

The author is very grateful to Prof. Arthur Rizzi for the support and encouragement and for always being generous with both time and money.

My fellow co-workers at the department and my fellow graduate students in the research group Simone and Hanyo and the already graduated Tomas are to be especially thanked.

Lastly and most importantly, I would like to thank my family and my girlfriend Helena for always being supportive and caring. Thank you!

Abstract

This thesis deals with the problems of scaling aerodynamic data from wind tunnel conditions to free flight. The main challenges when this scaling should be performed is how the model support, wall interference and the potentially lower Reynolds number in the wind tunnel should be corrected.

Computational Fluid Dynamics (CFD) simulations have been performed on a modern transonic transport aircraft in order to reveal Reynolds number effects and how these should be scaled accurately. This investigation also examined how the European Transonic Wind tunnel (ETW) twin sting model support influences the flow over the aircraft. In order to further examine Reynolds number effects a `MATLAB` based code capable of extracting local boundary layer properties from structured and unstructured CFD calculations have been developed and validated against wind tunnel measurements. A general scaling methodology is presented.

Licentiate Thesis

The thesis consists of an introduction and the following three papers:

Paper A

K. Pettersson and A. Rizzi, "Estimating Reynolds number scaling and wind-tunnel boom effects with the help of CFD methods", AIAA 2006, San Francisco USA, June 2006.

Paper B

K. Pettersson and A. Rizzi, "Reynolds number effects identified with CFD methods compared to semi-empirical methods", ICAS 2006, Hamburg Germany, September 2006.

Paper C

K. Pettersson and A. Rizzi, "Estimating local boundary layer properties using CFD and wind tunnel measurements", KTH Internal report 2006, Stockholm Sweden, September 2006.

Division of work between authors

Paper A

Pettersson performed the computations and wrote the paper. Rizzi supervised the work and contributed with valuable comments for the analysis of the results.

Paper B

Pettersson performed the computations and wrote the paper. Rizzi supervised the work and contributed with valuable comments for the analysis of the results.

Paper C

Pettersson performed the computations and wrote the paper. Rizzi supervised the work and contributed with valuable comments for the analysis of the results.

Contents

Chapter 1

Overview and summary

1.1 Background

Today are wind tunnel testing and CFD calculations natural and necessary parts in the development of an aircraft. The trends are that more and more time are spent both in the wind tunnel and performing CFD calculations. [19] This in order to avoid a costly step backwards to a previous design phase in order to correct potential mistakes. The main goal of the CFD calculations and the wind tunnel testing are to predict the free flight conditions of the aircraft. Accurate flight performance prediction is a challenging task because most of the testing has been done at sub-scale conditions. Some of the phenomena which has to be accounted for when scaling wind tunnel data to free flight condition are the wall and model support interference effects and potentially a lower Reynolds number. Some recent research on this topic is given by Eckert [9], where the influence of wall and sting interference and the impact of the propeller of the Airbus A-400M is investigated. The high cost associated with acquiring free flight test data makes the amount of information about scaling ground to flight methodology rare in the open literature and are often company proprietary and part of their competitive edge. [1] Some of the drivers of an increased accuracy in scaling methodology is the economical benefit from having an optimal choice of engine for a given aircraft configuration and the increased needs of reduction of emissions. [20] An erroneously predicted scale effect which would imply an increase in drag of 1% for an ultra high capacity aircraft would equate to around 3 tonnes of extra fuel at constant range or a reduction in range of 120 km for constant maximum take off weight. [22]

The scaling effects can introduce an element of risk in the aircraft programme, particularly for large wings, which are designed for high subsonic Mach numbers. An investigation of the scale and Reynolds number effects could increase the development costs drastically if they were to be done in the wind tunnel only. [20] Using CFD methods as a complement to wind tunnel testing can therefor be economically beneficial. Modern wind tunnel testing techniques and CFD methods also complement each other with the high fidelity of the wind tunnel results and the extensive data set (capable of free flight Reynolds and Mach number) from the CFD calculations enabling a thorough investigation of flow topology and phenomena.

Historically the importance of matching the free flight Mach number has never been in question. [22] Today it is also possible to match free flight Reynolds number in cryogenic facilities like the National Transonic Facility (NTF) [16] in USA and the European Transonic Wind tunnel (ETW) [10] in Europe. CFD methods and cryogenic wind tunnel testing are typically being incorporated early in the process when designing a modern transonic transport. The currently developed Boeing 787 was tested in the ETW early on in the design process and the final determination of how well the wind tunnel data matches flight performance will follow from flight testing in 2007-2008. [12]

The CFD calculations might not give the "right answer" in an absolute sense but they should perhaps be assumed to provide a solution within an acceptable accuracy bound. [27] It has however been pointed out that CFD is able to compute delta drag levels between similar configurations very well and that this was how CFD was generally used in industry for the design and development of aircraft. [14]

The wind tunnel correction is in question as well and should according to Rasuo [19] not be taken as the "exact value" and should not be accounted as the final result. The success of estimating scaling and Reynolds number effects has increased in later years due to the extensive use of cryogenic wind tunnels together with the use of modern CFD methods. [3]

A recent example of this is given by Nicoli [17] where the VEGA launcher (covering a wide range of Reynolds and Mach number) was scaled to free flight conditions using several different wind tunnels and modern CFD methods. Here a systematic error between CFD and wind tunnel results were identified, they were i.e. consistent with each other, and the two data sets could be regarded as one.

1.2 Scaling wind tunnel results

There could be several phenomena involved when scaling wind tunnel data to free flight condition and a classification of the phenomena involved is necessary in order to understand their effects and order of magnitude. This classification might be taken for granted by experienced wind tunnel users but it might serve a purpose to introduce it to the CFD community in order for them to classify numerical results with the same system and potentially identify differences between wind tunnel and CFD results.

One proposed classification of wind tunnel scaling effects is given by

Haines [13]. Here three different classes are pointed out; Scale effects, pseudo-Reynolds number effects and Reynolds number effects. The scale effects include such effects as model geometric fidelity or aeroelastic effects. The wind tunnel model might not have all the details (such as antennas and gaps etc) as the full scale aircraft and this will typically have an impact on the estimated drag of the aircraft. The aeroelastic effects are different when comparing the wind tunnel model, the full scale aircraft and the CFD model. In order to isolate pure Reynolds number effects (and keeping the aeroelastic effects constants in a cryogenic environment) one could keep the ratio of dynamic pressure to the models modulus of elasticity constant and vary Reynolds number, see Owens et al. [18] amongst others.

The pseudo-Reynolds number effects arise from effects which might at first glance seem to be a Reynolds number effect but at a closer inspection are found to be dependent on some other variable. The pseudo-Reynolds number effects are categorized into three main broad types according to Haines [13];

- Effects that arise when Reynolds number dependence are not allowed to vary within parameters or correction of test data, for example wind tunnel calibration and wall interference.
- When different data are being compared and Reynolds number is not the only dependent variable that is changing. Parameters like sound, heat or wind tunnel turbulence might also change with varying Reynolds number.
- Effects that are present because the test results are affected by some factor that might not be Reynolds number dependent but which is not similar to all data being compared; model surface finish or influence of the model support system.

The Reynolds number effects could in turn be categorized into direct and indirect Reynolds number effects. The direct Reynolds number effects are the ones associated with a constant pressure distribution while the indirect Reynolds number effects are associated with a change in pressure distribution for varying Reynolds number. In figure 1.1 are some of the direct and indirect Reynolds number phenomena of a wing profile shown.

Characteristics which are typically dependent on indirect Reynolds number effects are; lift and pitching moment, wave drag, drag divergence and buffet boundary. The characteristics which are dependent on direct Reynolds number effects on the other hand are typically; viscous drag, boundary layer separation and buffet boundary.

The well-known classical example of a Reynolds number effect which drastically made the transonic performance worse is the C-141. A plot of the super-critical pressure distribution and a schematic view of the boundary layer is shown in figure 1.2.

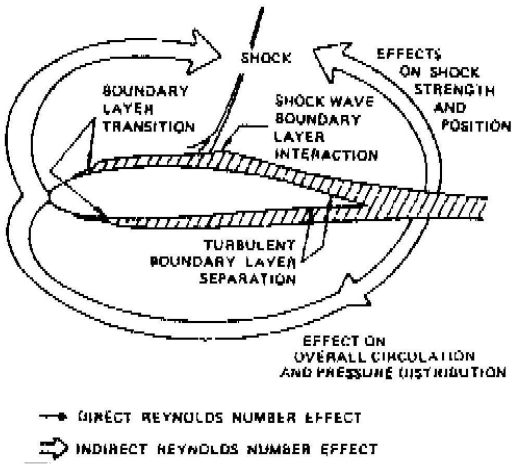

Figure 1.1: Schematic representation of direct and indirect Reynolds number effects on an airfoil, Vos et al. [26].

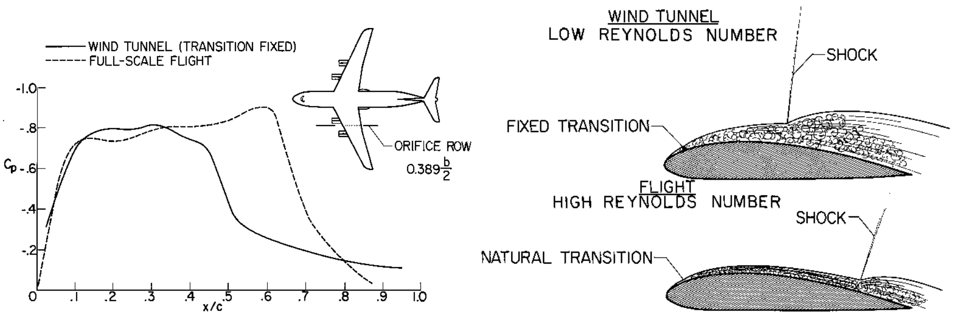

(a) Super critical pressure distribution.

(b) Schematic view of the boundary layer at wind tunnel and flight conditions.

Figure 1.2: Discrepancies in pressure distribution between wind tunnel and flight of the C-141, Blackwell [2].

In the wind tunnel the transition was fixed in the front of the airfoil and the agreement in transition position (in percent of chord-wise position) to the free flight condition was good. The larger Reynolds number at free flight conditions however made the relative thickness of the boundary layer smaller since the thickness of a turbulent boundary layer typically scales with $Re^{-1/5}$. This effect is shown in a schematic view in figure 1.2(b). The thinning of the boundary layer moves the shock wave in the stream-wise direction closer to the trailing edge. The region of shock induced separation has decreased in size. If C_L is kept constant for a given Mach number with increasing Reynolds number, the increased aft loading must be compensated with a decrease in the load over the front of the airfoil. This is generally accomplished by a decrease in the angle of attack. [7]

Saltzman [23] summarized in his work done in 1982, some of the known scaling issues at the time. The results for different aircraft and discrepancies between wind tunnel and flight conditions are shown in table 1.1

Table 1.1: Summary of wind tunnel model/flight discrepancies, Saltzman [23].

Aircraft	Discrepancy	Apparent cause	Remarks
P-51	Flight drag after pullout higher than for model	Different separation locations	Believe related to discussion of C-141 and M-2/F-3
X-5	Drag difference at Ma 1, though the same at drag divergence Ma	Chubby body, different separation locations	Probably differing afterbody flow
M-2/F-3	Base drag and boattail drag	Sting and different separation locations	Compensating effects; fortuitous
X-15	Base drag	Sting-affected base pressure	Eliminated variable by subtracting out
XB-70	Model drag too low at Ma 1.18	Tunnel wall effects	Flexibility effects may also have contributed
F-8	Second-velocity peak larger and farther aft in flight	Tunnel wall effects	Model too large, too close to Ma 1

Table 1.1 only serves as a summary of some different wind tunnel to flight discrepancies reported, for an extensive discussion see Saltzman [23], Haines [13] and Blackwell [2] amongst others. All of the discrepancies in table 1.1 occur at transonic speeds and are influenced by the following effects:

- Sting-support interference effects.
- Disproportionate boundary layer (Reynolds number effects).
- Wall interference effects.

The discrepancies noted in the C-141 example lead to the establishment of the trailing edge criterion, see Blackwell [2]. This was done in order to have a metric which one could compare wind tunnel results with fixed transition and free flight results with natural transition. The idea was that the transition strip should be moved so that the boundary layer thickness yielded a shock position which correlated with the results from flight tests. The use of shock position as metric in order to be able to compare two different cases could be replaced with some other simulation criteria. Haines [13] proposed the following:

- a zero-level criterion such as the boundary layer momentum thickness at the trailing edge of the equivalent flat plate, or
- a "first-order" criterion such as shock position, shock strength or the boundary layer momentum or displacement thickness at the trailing edge of the real wing, or
- a "second-order" or local criterion such as the boundary layer shape factor near the trailing edge of the non-dimensional length of a shock-induced separation bubble.

The simulation criterion would typically be located at a position where it had been influenced of the entire flow of the aircraft part investigated; the trailing edge in the case of the wing for example. This enables a comparison between a transition sweep and a Reynolds number sweep in order to investigate the viscous effects. The reoccurring issue of comparing CFD results with fully turbulent calculations and wind tunnel results with either fixed or free transition, could be investigated by inspection of one or more simulation criterion positioned in streamwise and spanwise position of the wing. The momentum thickness of a turbulent boundary layer is proportional to $Re^{-1/5}$ and the knowledge of the momentum thickness at two or more stream wise positions could reveal the transition position or information about potential differences between CFD, wind tunnel and free flight results.

A good candidate for trailing edge criterion except shock position and the length of a shock-induced separation would be a metric which is insensitive to measuring techniques in the wind tunnel or free flight. The integrated boundary layer properties like displacement thickness or momentum thickness are prone to be less sensitive to the specific measuring technique used or definition of boundary layer edge since potential errors have the possibility to even out. The approximately linear growth of Reynolds number based on momentum thickness (Re_θ) with increasing Reynolds number, as noted by Castillo [5] amongst others, makes it an attractive candidate. A difference in Re_θ for varying Reynolds number when comparing wind tunnel and CFD results could imply a change in indirect Reynolds number effects or transition positions.

In figure 1.3 are Re_θ vs. Reynolds number shown using data from the wind tunnel campaign performed by Degraaff [8]. In the wind tunnel campaign the flow over a swept bump was analyzed using different measuring techniques. Three different stream-wise positions ranging from the mid part to the trailing edge of the swept bump is shown. The two lower Reynolds numbers are performed at 1 atm pressure with low and high free stream velocities (approximately 5 and 15 m/s) while the two higher Reynolds number conditions are performed at 4 and 8 atm pressure conditions with a free stream velocity of approximately 15 m/s. All cases were carried out at temperature close to room temperature (300 K) and with fixed transition. The approximately linear growth is seen in figure 1.3, where the slope of

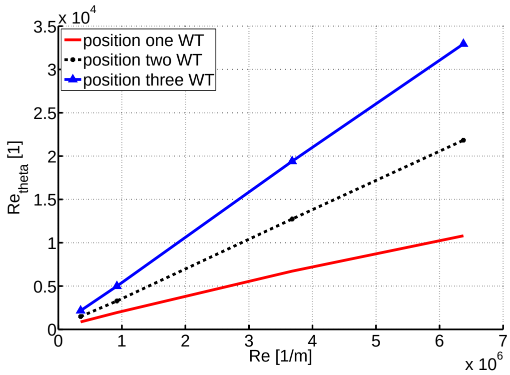

Figure 1.3: Re_θ vs. Re for three different positions with varying pressure gradients, data from Degraaff [8].

the curves are dependent on the local pressure gradient. The root mean square of the errors between a linear fit and the wind tunnel results are 150, 50 and 110 for positions one, two and three respectively (where the order of magnitude of Re_θ is 10^4). A sudden divergence from the linear growth would typically imply a change in pressure distribution or shock strength. The Reynolds number where this divergence would appear could then be used to identify a critical Reynolds number.

An early attempt to incorporate CFD calculations to Reynolds number scaling of wind tunnel results was performed by Reichenbach and McMasters [21]. Here the inviscid, two dimensional results from CFD calculations was regarded as the limiting result of Reynolds number going to infinity. This gave an extra data point far away from the low Reynolds number wind tunnel results, which made it possible to scale the data. Today viscous calculations of full aircraft configurations using the RANS equations are performed almost on a daily basis. This might give extra information about Reynolds number effects and trends. The impact of varying transition positions or identifying compressible effects for varying Reynolds number could be evaluated using Re_θ as trailing edge criterion when comparing wind tunnel, CFD and free flight results.

According to Saltzman [23] has some of the most decisive and useful tunnel-to-flight correlations resulted from the local aerodynamics experimental approach wherein the aerodynamic characteristics of a single component are defined, in contrast to evaluating the performance of the entire airplane at once. Therefore an investigation of the trailing edge criterion at one or more positions of the different aircraft components investigated is recommended when analyzing the viscous effects. This in order to identify scaling or Reynolds number effects for each part of the aircraft separately, which might cancel out when global drag is examined.

1.2.1 Wind tunnel wall and model support interference

In all wind tunnel correction methodologies both the wind tunnel wall and the model support system has to be taken into account. In the REMFI project [11] flow phenomena on the empennage was investigated. This included effects such as horizontal tail plane (htp) stall, gap effects and scale effects. A twin sting support system (see figure 1.4) was used in the ETW in order to examine the empennage drag using a "live rear-end" measuring technique at high Reynolds number. In the wind tunnel campaign both wings on/off and tail on/off were evaluated. In figure 1.4(a) is the aircraft mounted without tail plane in the ETW, while in figure 1.4(b) has the tail plane been added. CFD calculations performed with the support system on and off could reveal potential scaling effects of the live rear end drag measurements.

(a) Aircraft mounted in the ETW with a twin sting support (courtesy of ETW, [10]).

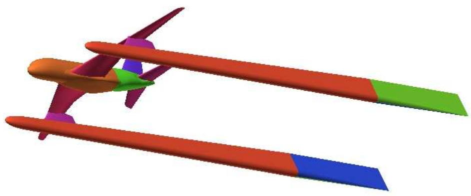

(b) CAD representation of the aircraft and twin sting support.

Figure 1.4: Wind tunnel model and the CAD representation to be used as input in CFD calculations.

Another modern example showing the success of integrating wind tunnel and CFD calculations is the work of Melber-Wilkending et al. [15]. In this work the wind tunnel walls interference effects were evaluated using CFD methods. The model mounted in the wind tunnel and the model in free flight were calculated and compared.

1.2.2 Scaling Drag with Reynolds number

Using a high performance but also high cost facility like the ETW in a cost efficient manner is an art in itself, see Griffiths and Wright [12]. Even if a successful wind tunnel campaign has been conducted the data must be corrected for wind tunnel wall and support system interference and a scaling of the aerodynamic coefficients to free flight conditions. In figure 1.5 are the ETW capabilities shown where it is obvious that some scaling of the full-span models to free flight Reynolds number must be conducted.

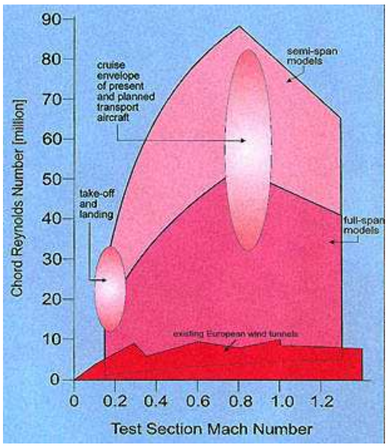

Figure 1.5: ETW capabilities (courtesy of ETW, [10]).

One way of extrapolating drag is to anchor the highest available Reynolds number drag data to a flat plate semi empirical function relating skin friction with Reynolds number. The function describing the skin friction could either be based on laminar or turbulent flow. One could also use both of the laminar and turbulent skin friction functions in proportions to how much laminar and turbulent flow one assumes at free flight conditions (see Tomek et al. [25] and Wahls et al. [28] amongst others).

According to Covert [6] the wind tunnel drag data could be anchored to the semi empirical method by multiplication of a constant, where the constant would correspond to effects such as interference, drag due to pressure and wave drag etc. Two commonly used skin friction relations are given in Covert [6]; the Prandtl-Schlichting, equation (1.1), and the Karman-Shoenherr, equation (1.2).

$$C_F = \frac{0.455}{\log_{10}(Re)^{2.58}} - A/Re \tag{1.1}$$

The constant A in equation (1.1) is dependent on at which Reynolds number transition is assumed to occur. There are however questions how accurate equation (1.1) is for higher Reynolds number and care should be taken when the Reynolds number is larger than 10^7.

$$\frac{0.242}{\sqrt{C_F}} = \log_{10}(C_F \cdot Re) \tag{1.2}$$

Both of the skin friction relations are derived for incompressible flow. In Carlson [4] are several methods of transforming incompressible skin friction to a compressible form presented. In the work of Carlson [4], it is shown that the T' and the van Driest II methods are the ones which collapses the transformation to compressible skin friction best. In this thesis has the Sommer-Short T' method (see Sommer and Short [24] for further details) been evaluated. By following the cook book recipe presented by Sommer and Short [24] and using the Sutherland formula for viscosity the skin friction could be transformed to a compressible state in the following manner:

Firstly the temperature ratio is calculated using equation (1.3) and a recovery factor (r) equal to 0.89 (which should be in good agreement with experimental results of turbulent flow according to White [29]).

$$\frac{T_{wall}}{T_\infty} = 1 + r \cdot (\frac{\gamma - 1}{2}) \cdot Ma^2 \tag{1.3}$$

The intermediate state, the T' state is then calculated using equation (1.4).

$$\frac{T^{'}}{T_\infty} = 1 + 0.035 \cdot Ma^2 + 0.45 \cdot (\frac{T_{wall}}{T_\infty} - 1) \tag{1.4}$$

When T' and T_∞ are known the corresponding $Re^{'}$ could be evaluated assuming constant pressure through the boundary layer and Sutherland's formula, see equation (1.5).

$$Re^{'} = \frac{Re}{(\frac{T^{'}}{T_\infty})^{5/2} \cdot (\frac{T_\infty + S}{T^{'} + S})} \tag{1.5}$$

$C_F^{'}$ is then calculated using once favorite skin friction method, equation (1.2) for instance, with $Re^{'}$ from equation (1.5).

Finally the compressible skin friction is given by using equation (1.6).

$$C_{F,comp.} = \frac{C_F^{'}}{T^{'}/T_\infty} \tag{1.6}$$

Figure 1.6, shows the results of the Karman-Shoenherr and Sommer-Short methods predicting compressible skin friction trends.

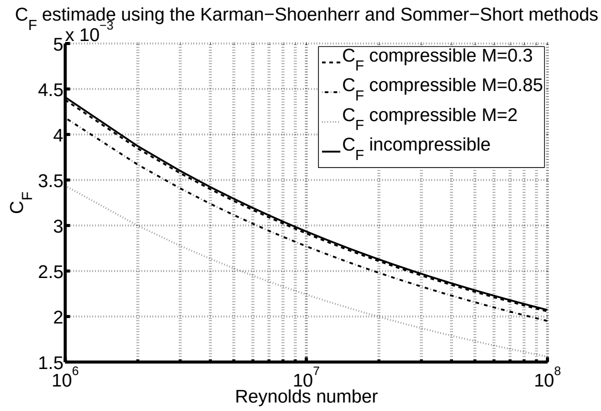

Figure 1.6: Compressible and incompressible skin friction estimated using the Karman-Shoenherr and Sommer-Short methods.

The extrapolation methodology used in the work of Nicoli et al. [17] is presented as a final example of how CFD and wind tunnel data could serve as means to scale aerodynamic data to flight conditions. The object investigated was the VEGA, a new European small launcher. CFD calculations were performed using the ZEN code. The wind tunnels used in order to cover the wide range in Reynolds and Mach number were the T1500 used by FOI in Sweden for the subsonic and transonic regime, the SST used by DNW the German-Dutch wind tunnels in the supersonic regime and finally the H2K used by DLR in Germany in the hypersonic regime.

At each Mach number, the trends in aerodynamic coefficients were approximated by equation (1.7).

$$C_X = a \cdot (\log_{10}(Re))^{b(M,\alpha)} \tag{1.7}$$

C_X in equation (1.7) could be either the normal, the axial or the tip moment coefficient. The constants a and b were fitted to the wind tunnel/CFD data set and b were allowed to vary as a function of Mach number and angle of attack.

1.3 New general scaling methodology

According to Haines [13] understanding the flow is a better maxim than using the old numbers for scaling methodology. Keeping this in mind when scaling aerodynamic data and to be able to estimate interference effects, the following procedure is recommended;

- Compare the CFD and wind tunnel data using the trailing edge criterion, oil flow topology and integrated forces and moments.

- Are there any systematic errors present? If there are, correct the data sets and regard them as consistent. If the discrepancies are inconsistent, could this be explained?
- Could a critical Reynolds number be observed? Does the wind tunnel and CFD critical Reynolds number match? If not, could this be explained?
- Decide the order of magnitude of potential flow phenomena occurring above wind tunnel Mach or Reynolds number capabilities with the help of trailing edge criterion, oil flow topology and integrated forces and moments from the CFD calculations.
- If wind tunnel and CFD results have shown to be consistent at lower Reynolds number, scale the wind tunnel aerodynamic data set using the constant discrepancy between the CFD and wind tunnel results shown at lower Reynolds number to flight conditions calculated with the CFD methods.

The purpose of the procedure presented is to make a close comparison between CFD and wind tunnel results in order to understand and visualize the different flow phenomena occurring for a given aircraft configuration. A better understanding of the effects of potentially differing transition positions between wind tunnel and CFD calculations, an identification of critical Reynolds number and evaluation of interference effects could be the benefit of using this procedure.

When scaling wind tunnel drag to a higher Reynolds number the pressure drag and viscous drag could be evaluated by using the ratio of skin friction drag to drag due to pressure from the CFD calculations. Once the order of magnitude of viscous and pressure drag from the wind tunnel is known, they could be scaled separately. Scaling only viscous drag with semi-empirical skin friction methods will typically yield a more accurate result than scaling the complete drag all at once. The Karman-Shoenherr and Sommer-Short method for scaling skin friction has proven to yield reliable results even for very high Reynolds number data and is therefore recommended. Scaling drag due to pressure with varying Reynolds number was found to correlate better with a power-law function of the type $C_{D_P} = C_1 + C_2(Re)^n$, for the attached flow of the aircraft investigated. The three constants need to be determined from three wind tunnel results with as large difference in Reynolds number as possible in order to make the problem of fitting the data well conditioned.

Chapter 2

Summary of papers

Paper A

Here the isolated interference effects of the twin sting boom in the ETW is evaluated. The investigation was done at low angle of attack, transonic Mach number and for varying Reynolds number. The booms were shown to have a small influence on the empennage drag.

Paper B

Different scaling techniques of drag for varying Reynolds number for a modern transonic aircraft is presented. Scaling skin friction and drag due to pressure separately was presented as a methodology with good potentials for high accuracy in drag scaling. Skin friction was scaled using the Karman-Shoenherr and Sommer-Short methods and drag due to pressure with a novel formulation. The correlation between the extrapolated drag and CFD results at higher Reynolds number were good. It was shown that the CFD calculations using the RANS equations were capable of predicting a linear growth in Reynolds number based on momentum thickness for a full scale aircraft configuration with mainly attached flow.

Paper C

CFD calculations with two different codes and two different turbulence models were performed in order to investigate local boundary layer properties and how these correlated with wind tunnel measurements. The wind tunnel model consisting of channel flow and a swept bump was evaluated in order to analyze the three dimensional and pressure gradient effects of the flow. A `MATLAB` code capable of extracting local boundary layer properties from CFD calculations done on structured and unstructured meshes were developed and validated. The overall match between CFD and wind tunnel results were good but the `Edge` code using the Spalart-Allmaras model showed to be the most promising solution for this attached flow case topology.

Chapter 3

Conclusions and future work

A Reynolds number investigation of a modern transonic transport at cruise condition has been performed using CFD methods. The Reynolds number dependence of drag and separation has been evaluated. Small regions of Reynolds number dependent separation were found. A new general scaling methodology is proposed. Scaling viscous drag and pressure drag separately yielded a more accurate result than scaling them both at once. Viscous drag was scaled with the Karman-Shoenherr and Sommer-Short methods and pressure drag was scaled with a novel formulation. The ETW model support used in this project, a twin sting arrangement, had a small influence on the empennage drag. A `MATLAB` based code able of evaluating local boundary layer characteristics were developed and validated against wind tunnel results. Local boundary layer Reynolds number effects were investigated comparing different wind tunnel measuring techniques and CFD methods. Two CFD codes and two turbulence models were evaluated and the overall agreement between CFD and wind tunnel results were good. Using the trailing edge criterion as a metric for comparisons of CFD and wind tunnel results in order to scale aerodynamic data to free flight condition seems to be a valuable tool.

The intention is to continue this research in pursuit of the doctoral degree. This work will then continue in three general directions. The continued use of CFD methods to compute several more flight cases with respect to sweep in angle of attack, Reynolds number and Mach number are scheduled. A close comparison and analysis between the CFD results and wind tunnel data from the ETW and ARA wind tunnels are to be conducted. Further analysis of the scaling techniques at take-off, cruise and landing configurations are planned.

References

[1] Jewel B. Barlow, William H. Rae, and Alan Pope. *Low-Speed Wind Tunnel Testing*. Wiley-Interscience, 3 edition, 1999.

[2] James A. Blackwell. Preliminary study of effects of reynolds number and boundary-layer transition location on shock-induced separation. *NASA*, January 1969.

[3] Dennis M. Bushnell. Scaling: Wind tunnel to flight. *Annual Review of Fluid Mechanics*, 38:111–128, 2006.

[4] John R. Carlson. Prediction of very high reynolds number compressible skin friction. *AIAA*, 1998.

[5] Luciano Castillo. *Similarity Analysis of Turbulent Boundary Layers*. PhD thesis, State University of New York at Buffalo, February 1997.

[6] Eugene E. Covert. Thrust and drag: Its prediction and verification. In *Progress in Astronautics and Aeronautics Series*, volume 98. AIAA, 1985.

[7] A. Crook. Skin-friction estimation at high reynolds numbers and reynolds-number effects for transport aircraft. In *Annual Research Briefs*, pages 427–438. Center for Turbulence Research, 2002.

[8] David B. DeGraaff. *Reynolds number scaling of the turbulent boundary layer on a flat plate and on swept and unswept bumps*. PhD thesis, Stanford University, January 1999.

[9] D. Eckert and G.H. Hegen. Dnw's method to correct for support and wall interference effects on low speed measurements with a large propeller powered transport aircraft model. *ICAS*, 2006.

[10] ETW. Etw. http://www.etw.de, September 2006.

[11] European Comission, editor. *Aeronautics Research 2003-2006 projects*, volume Project synopses - volume 1 Research Projects from the first and second calls. Office for Official Publications of the European Communities, 2006.

[12] Robert C. Griffiths and Martin C. N. Wright. Performance testing with high productivity in a low speed flight reynolds number test campaign. *ICAS*, 2006.

[13] A. B. Haines. Scale effects on aircraft and weapon aerodynamics. In *AGARD-AG-323*. AGARD, 1994.

[14] Kelly R. Laflin. Aiaa cfd drag prediction workshop: An overview. *ICAS*, 2006.

[15] S. Melber-Wilkending, A. Heidelbrecht, and G. Wichmann. A new approach in cfd supported wind tunnel testing. *ICAS*, 2006.

[16] NASA. Ntf. http://windtunnels.larc.nasa.gov, September 2006.

[17] A. Nicoli, B. Imperatore, M. Marini, and P. Catalano. Ground-to-flight extrapolation of the aerodynamic coefficients of the vega launcher. *AIAA*, June 2006.

[18] L.R. Owens and R.A Wahls. Reynolds number effects on a supersonic transport at subsonic high-lift conditions. *AIAA*, 2001.

[19] Bosko Rasuo. On status of wind tunnel wall correction. *ICAS*, 2006.

[20] Daniel Reckzeh and Heinz Hansen. High reynolds-number windtunnel testing for the design of airbus high-lift wings. In *New Results in Numerical and Experimental Fluid Mechanics V*, pages 1–8. Springer, 2006.

[21] S.H. Reichenbach and J.H. McMasters. A semiempirical interpolation technique for predicting full-scale flight characteristics. *AIAA-87-0427*, January 1987.

[22] Stepehn Rolston. High reynolds number tools and techniques for civil aircraft desing. *AIAA*, June 2001.

[23] Edwin J. Saltzman and Theodore G. Ayers. Review of flight-to-wind-tunnel drag correlation. *Journal of Aircraft*, 19(10):801–811, October 1982.

[24] Simon C. Sommer and Barbara J. Short. Free-flight measurements of turbulent-boundary-layer skin friction in the presence of severe aerodynamic heating at mach numbers from 2.8 to 7.0. *NACA-TN-3391*, March 1955.

[25] W.G. Tomek, R.A. Wahls, L.R. Owens, A.B. Burner, S.S. Graves, and J.M. Luckring. Investigation of aerodynamic scale effects for a generic fighter configuration in the national transonic facility. *AIAA*, January 2003.

[26] J.B. Vos, A. Rizzi, D. Darracq, and E.H. Hirschel. Navier-stokes solvers in european aircraft design. In *Progress in Aerospace Sciences*, pages 601–697. Elsevier, 2002.

[27] Bernd Wagner, Michael Mifsud, Jason Bennett, and Scott Shaw. Numerical computation of the x-15 wind tunnel and flight experiments: A validation and verification case study. *ICAS*, 2006.

[28] R.A Wahls, L.R. Owens, and S.M.B Rivers. Reynolds number effects on a supersonic transport at transonic conditions. *AIAA*, 2001.

[29] Frank M. White. *Viscous Fluid Flow.* Mechanical Engineering. McGraw-Hill, second edition, 1991.